

Terrain-Aware Foot Placement for Bipedal Locomotion Combining Model Predictive Control, Virtual Constraints, and the ALIP

Grant Gibson, Oluwami Dosunmu-Ogunbi, Yukai Gong, and Jessy Grizzle

Abstract—This paper draws upon three themes in the bipedal control literature to achieve highly agile, terrain-aware locomotion. By terrain aware, we mean the robot can use information on terrain slope and friction cone as supplied by state-of-the-art mapping and trajectory planning algorithms. The process starts with abstracting from the full dynamics of a Cassie 3D bipedal robot, an exact low-dimensional representation of its centroidal dynamics, parameterized by angular momentum. Under a piecewise planar terrain assumption, and the elimination of terms for the angular momentum about the robot’s center of mass, the centroidal dynamics become linear and has dimension four. Four-step-horizon model predictive control (MPC) of the centroidal dynamics provides step-to-step foot placement commands. Importantly, we also include the intra-step dynamics at 10 ms intervals so that realistic terrain-aware constraints on robot’s evolution can be imposed in the MPC formulation. The output of the MPC is directly implemented on Cassie through the method of virtual constraints. In experiments, we validate the performance of our control strategy for the robot on inclined and stationary terrain, both indoors on a treadmill and outdoors on a hill.

I. INTRODUCTION

This paper contributes to the growing literature on terrain-aware, also known as terrain-adaptive, locomotion. Our objective is to design a gait controller that enables an agile bipedal robot, such as Cassie in Fig. 1, to traverse terrain that is varying in height and surface friction at “speed”, meaning locomotion “as close to the planned velocity as the physical limits of the robot and terrain allow”. We will assume that the robot is provided a local map that specifies (a) terrain height, that is, z as a function of x and y in a region about the robot, and (b) a C^1 vector field of desired velocity (speed, heading, and yaw rate) as a function of the robot’s current pose and velocity. The integral curves of the vector field provide a family of paths that the robot may follow to reach a goal that is unknown to the local gait controller. The vector field may come from a reactive planner, as in [1], [2], or through a human operator and an RC-controller, as in this paper.

We make a key simplifying assumption on the terrain, namely, that over distances on the order of the step length of the robot, it can be piecewise approximated by planes, with allowed jumps at the boundaries. This admittedly vague assumption will be made more precise in Sect. II, where we model the centroidal dynamics of the robot. The gait controller will plan N robot-steps ahead, where N is a small number such as four, and will assume that beyond this planning horizon, the terrain is flat with a nominal friction

The authors are with the College of Engineering and the Robotics Institute, University of Michigan, Ann Arbor, MI 48109 USA
 {grantgib, grizzle}@umich.edu

coefficient. More realistic assumptions on the terrain beyond the gait-controller’s planning horizon will be made in the near future when this controller is integrated with the reactive planner and a full perception and mapping system introduced in [3], [4]. The length of the gait-controller’s planning horizon is limited by the need for real-time computations with a model that contains more information on dynamics and constraints than is currently used in trajectory/motion planning methods.

A. Related Work

Blurring the Boundary between Gait Control and Trajectory Planning: As emphasized in [5], the separation of vehicle control into independently designed path planner and a low-level “speed and direction” controller inevitably results in performance degradation. The proposed remedy was an integrated system based on Model Predictive Control (MPC). Related work in the area of legged robots includes the quadrupedal robot Anymal B in [6], which achieves terrain-aware foothold planning by tightly coupling locally optimal footholds and center of mass velocity with a terrain height map. The authors show how to voxelize the terrain map and perform a real-time grid search to optimize foot placement.

Switching Control Based on One-step Ahead Terrain Profile: Terrain aware locomotion of a simulated 3D humanoid is achieved in [7]. First, in an offline stage, a library is built that includes five periodic gaits and a set of transition gaits



Fig. 1: Cassie Blue using a 3D-ALIP inspired MPC foot placement controller to walk sideways up a 22° incline on wet grass. Lateral walking with Cassie is much more difficult than longitudinal walking due to tight workspace constraints, which are accounted for in our formulation.

that terminate in a periodic gait. The gaits are parameterized so as to allow a low-level joint controller to move the robot in a single step from a current pose to a desired final pose, with the desired pose planned in real-time at step initiation as a function of a terrain height map. In a similar vein, reference [8] first develops a set of feedback controllers for bipedal walking on flat ground, upstairs and downstairs, called motion primitives. In a second step, a set of feedback controllers is designed that evolve the robot from one motion primitive to another (termed motion transitions). The appropriate controller is selected at step transition.

Terrain Robust: Other locomotion work is “terrain aware” in a quite different sense: when the gait controller is being designed, it is challenged with a finite set of terrain height perturbations [9]–[12]. During offline optimization, which could be via parameter optimization or reinforcement learning, a “score” is assigned based on how the closed-loop system (consisting of the controller and robot) responds to a family of terrain profiles, “knowing that” online, the controller is only allowed to use proprioception (such as IMU and joint encoder signals) to complete a locomotion task. In particular, the controller is not provided exteroceptive information on terrain profile, as in the previous work we reviewed.

MPC for Foot Placement without Terrain Preview: In [13], the decoupled Linear Inverted Pendulum (LIP) model dynamics, first introduced in [14], is used to solve a hybrid system-based optimization problem by computing center of pressure trajectories for a specified footfall pattern. These trajectories are computed at the beginning of each domain and are used as inputs to a virtual constraint-based quadratic program to realize joint torque commands. A separate hybrid system and MPC approach was performed in [15] for computing footfalls on a bipedal robot. The footfalls were chosen in order to minimize the error between the propagated LIP dynamics and a pre-specified reference trajectory.

One Step-Ahead Prediction: This paper adapts the philosophy of [5] and designs an MPC controller that blurs the boundary between gait generation and trajectory planning. Our starting point is the one-step ahead gait controller in [16], [17], which bridged the gap between the low-dimensional linear inverted pendulum (LIP) models in [14], [18]–[22] and the method of Virtual constraints and Hybrid Zero Dynamics in [11], [23], [24]. The key was to model the centroidal dynamics of a physical robot in terms of *angular momentum about the contact point*. A four dimensional linear model (referred to as the 3D-ALIP) resulted when a 3D bipedal robot was controlled such that its center of mass height was constant and the angular momentum about its center of mass had a negligible effect over a step. When the center of mass height was constant, the four dimensional model decoupled into two 2D models for the sagittal and frontal planes, respectively.

These models were subsequently used to predict forward in time the angular momenta at the end of the next step as a function of the robot’s current angular momenta, position of its center of mass, and the swing-foot position at the

end of the current step. When a (dead-beat) foot-placement controller was designed to place the swing foot so as to match the predicted angular momentum to desired angular momentum at the end of the next step, the Cassie bipedal robot was able to walk at 2.1 m/s, complete a 90° turn in 5 steps when walking at 1 m/s, and traverse significant slopes [4].

Importantly, *achieving this agile performance on Cassie required a skilled operator for the RC controller*, an operator who would not command the robot to “accelerate too quickly” or “turn too quickly”, and would “appropriately adjust foot clearance” before walking on 22° slopes. The current paper will transform the one-step ahead controller in [16] into a full-blown multi-step horizon MPC controller. Moreover, the center of mass will not be limited to a constant height, workspace constraints on the legs will be included during the step to avoid collisions with one another as well as unwanted contacts with the ground, and finally, the friction cone of the local terrain can be included.

B. Contributions

We provide the following contributions for enhancing terrain-aware locomotion:

- Derive the exact centroidal dynamics of a bipedal robot with contact assuming the center of mass moves on a plane that need not be parallel to the ground. We explicitly choose angular momentum as a state over linear velocity and justify why the resulting dynamics can be decoupled from the angular momentum about the centroid and yaw axis.
- Create a novel set of virtual constraints which can be used on a bipedal robot to track the desired motion of the aforementioned reduced-order dynamics for locomotion on piecewise linear terrain.
- Formulate an N-step receding horizon optimization problem which incorporates the 3D-ALIP dynamics and terrain-aware workspace constraints for computing foot placement to converge to desired periodic trajectories.
- Implement this control algorithm on a high degree-of-freedom 3D bipedal robot (Cassie).

II. 3-D ROBOT MODELS

A. 3D Physical Robot Model

We assume a pinned point contact dynamic model of the form

$$D(q)\ddot{q} + C(q, \dot{q})\dot{q} + G(q) = B(q)u, \quad (1)$$

with no yaw motion about the stance foot (Cassie has a blade foot). The generalized coordinates $q \in \mathbb{R}^n$, the vector of motor torques $u \in \mathbb{R}^m$, and the torque distribution matrix has full column rank. For Cassie, $n = 15$ due to the blade foot and $m = 10$ if the ankle torque on the stance foot is included. In this work, it will be set to zero, leaving $m = 9$.

B. Centroidal Dynamics for Full-Order and Reduced-Order Model

For a 3D robot with a point contact, the dynamics for CoM positions and angular momenta about the contact point can be written as follows,

$$\begin{aligned}\dot{x}_c &= \frac{L^y}{mz_c} + \frac{\dot{z}_c}{z_c} x_c - \frac{L_c^y}{mz_c} \\ \dot{y}_c &= -\frac{L^x}{mz_c} + \frac{\dot{z}_c}{z_c} y_c + \frac{L_c^x}{mz_c} \\ \dot{L}^x &= -mgy_c \\ \dot{L}^y &= mgx_c.\end{aligned}\quad (2)$$

where x_c, y_c, z_c denote the CoM position, $L^{x,y,z}$ denote the angular momenta about the x, y, z -axes of the contact point.

Motivated by the parallel height constraint from the LIP model [25], we introduce the following constraints,

$$\begin{aligned}z_c &= k_x x_c + k_y y_c + z_H \\ \dot{z}_c &= k_x \dot{x}_c + k_y \dot{y}_c,\end{aligned}\quad (3)$$

under which the model becomes

$$\begin{aligned}\dot{x}_c &= \frac{L^y}{mz_H} + \frac{k_y}{z_H} (x_c \dot{y}_c - y_c \dot{x}_c) - \frac{L_c^y}{mz_H} \\ \dot{y}_c &= -\frac{L^x}{mz_H} - \frac{k_x}{z_H} (x_c \dot{y}_c - y_c \dot{x}_c) + \frac{L_c^x}{mz_H} \\ \dot{L}^x &= -mgy_c \\ \dot{L}^y &= mgx_c.\end{aligned}\quad (4)$$

The slope of the x and y ground planes are represented by $k_x = \tan \alpha_x$ and $k_y = \tan \alpha_y$, respectively. By the equation $L = L_c + [x_c, y_c, z_c]^T \times m [\dot{x}_c, \dot{y}_c, \dot{z}_c]^T$, the above can be rewritten to make L^z explicit,

$$\begin{aligned}\dot{x}_c &= \frac{L^y}{mz_H} + \frac{k_y}{mz_H} (L^z - L_c^z) - \frac{L_c^y}{mz_H} \\ \dot{y}_c &= -\frac{L^x}{mz_H} - \frac{k_x}{mz_H} (L^z - L_c^z) + \frac{L_c^x}{mz_H} \\ \dot{L}^x &= -mgy_c \\ \dot{L}^y &= mgx_c.\end{aligned}\quad (5)$$

In [17], it has been shown that both L_c^x and L_c^y are small compared to L^x and L^y , respectively. By using L^x and L^y as state variables in place of the CoM velocities, neglecting L_c has only a small effect on the dynamic accuracy during normal walking, even for robots with *heavy* legs.

Next, we make the case that $(L^z - L_c^z)$, which is the same as $(x_c \dot{y}_c - y_c \dot{x}_c)$, can be neglected. Some readers might already believe $(L^z - L_c^z)$ is a small term. For others, there are two ways to look at it intuitively: 1) When a robot is walking purely longitudinally ($y_c = \dot{y}_c = 0$) or laterally ($x_c = \dot{x}_c = 0$) the product is zero. For diagonal movement, we can define a new frame aligned with the walking direction, which also makes the y_c and \dot{y}_c terms small. 2) If we project the position vector and velocity vector to a horizontal plane, then $(x_c \dot{y}_c - y_c \dot{x}_c)$ is the cross product of these two projected vectors. Throughout a walking gait, either the angle between the two projected vectors is small or the magnitude of the projected position vector is small.

As a result of these approximations, we arrive at the dynamics for the 3D-ALIP model with center of mass evolving as in (3),

$$\dot{\mathbf{x}} = \begin{bmatrix} \dot{x}_c \\ \dot{y}_c \\ \dot{L}^x \\ \dot{L}^y \end{bmatrix} = \underbrace{\begin{bmatrix} 0 & 0 & 0 & \frac{1}{mz_H} \\ 0 & 0 & -\frac{1}{mz_H} & 0 \\ 0 & -mg & 0 & 0 \\ mg & 0 & 0 & 0 \end{bmatrix}}_A \begin{bmatrix} x_c \\ y_c \\ L^x \\ L^y \end{bmatrix}. \quad (6)$$

We reiterate that the state includes the angular momenta rather than the center of mass velocities; the benefits of this selection have been highlighted in several related works [11], [16], [26], [27]. An additional insight is that the velocities are coupled to the yaw torque of the system. By inspection this yaw torque, L_z is a pure integrator and, as shown in the next section, is uncontrollable through foot placement.

C. Foot Placement as a Control Variable

The dynamic model (6), which describes the evolution of the centroidal dynamics when the robot is in single support, is not affected by the motor torques¹. So how to control it? As in [16], [27]–[29], we use the placement of the end of the swing leg as a step-to-step actuator. Under conservation of angular momentum and (3), if \mathbf{x}^- is the solution of (6) just before impact, and \mathbf{x}^+ is the value of the state just after the (instantaneous) impact, then

$$\mathbf{x}^+ = \mathbf{x}^- + B \mathbf{u}_{fp}, \quad (7)$$

where

$$B = \begin{bmatrix} -1 & 0 & 0 & 0 \\ 0 & -1 & 0 & 0 \end{bmatrix}^T \quad (8)$$

and \mathbf{u}_{fp} is the resultant vector emanating from the current stance contact point to the desired swing foot impact location.

We assume that the height of the swing leg is controlled so that the duration of each step of the robot is fixed at T_s . Hence, during the k -th step of the robot, the height of the swing leg above the ground is regulated to be positive for $(k-1)T_s < t < kT_s$ and zero at kT_s . The relative (x, y) position of the swing leg end at time kT_s is selected so as to achieve a desired evolution of (6) for $t > kT_s$.

III. MPC FORMULATION FOR FOOT PLACEMENT CONTROL OF 3D-ALIP

In [16], $\mathbf{u}_{fp}(kT_s)$ was selected step-to-step to achieve a desired value of the angular momenta in (6) at time $(k+1)T_s$, in other words, at the end of the next step. The values of x_c and y_c were not regulated. One-step ahead foot placement as in [16] can be viewed as MPC with a terminal linear equality constraint on a portion of the state vector and no inequality constraints. Here, we will give an MPC formulation of foot placement control over a multi-step horizon, a quadratic cost to be minimized, and appropriate linear inequality constraints to make the solution terrain aware.

¹Recall that we are purposefully leaving the stance ankle passive in this study.

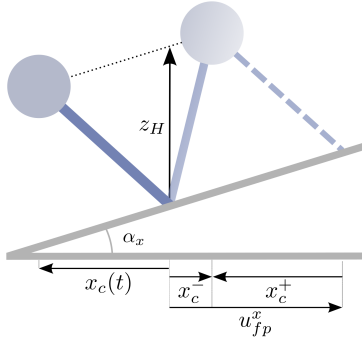


Fig. 2: The planar linear inverted pendulum is shown. $x_c(t)$ represents the location of the center of mass with respect to the stance foot at time t . The control input u_{fp}^x denotes the foot placement at the end of the current step. The state before and after instantaneous impact is denoted with a minus and plus sign, respectively.

We begin by defining

- N_s , the number (robot) steps of (fixed) duration T_s in the MPC control horizon.
- $\delta t = T_s/M$ is the sample period for the controller, where $M > 1$ is an integer.
- $A_\delta := \exp(A\delta t)$, the state transition matrix of (6) for a time duration of δt seconds.
- \mathbf{x}_0 in the MPC will always be the predicted solution $\hat{\mathbf{x}}(kT_s, t)$ of (6) just before impact, based on the measured value of state at time t , that is,

$$\mathbf{x}_0 := \hat{\mathbf{x}}(kT_s, t) := \exp(A(kT_s - t))\mathbf{x}(t). \quad (9)$$

This will allow us to work with a fixed control horizon.

- With the above in hand, we define the discrete-time dynamics

$$\mathbf{x}_{i+1} = \begin{cases} A_\delta(\mathbf{x}_i + B\mathbf{u}_{fp,i}) & , i \in \{0, M, 2M, \dots, (N_s-1)M\} \\ A_\delta\mathbf{x}_i & , \text{otherwise} \end{cases} \quad (10)$$

for use in our MPC problem as it will allow us to place constraints on the intra-step evolution of $x(t)$, that is, its behavior between steps

- $\mathbf{x}_i^{\text{des}}$ is the desired evolution of the state and the associated error term is

$$\mathbf{x}_{e,i} := \mathbf{x}_i - \mathbf{x}_i^{\text{des}}. \quad (11)$$

A. MPC Problem

An N_s -step horizon MPC control problem with quadratic cost and linear constraints can now be formulated as

$$\begin{aligned} \min_{\mathbf{U}_{fp}} J = & \sum_{i=0}^{MN_s-1} \mathbf{x}_{e,i}^T Q_i \mathbf{x}_{e,i} + \mathbf{x}_{e,MN_s}^T Q_f \mathbf{x}_{e,MN_s} \\ \text{subject to} & \end{aligned} \quad (12)$$

(9), (10), and (11)

$$\forall \mathbf{x}_i \in \mathcal{X} \text{ and } \forall \mathbf{u}_{fp,i} \in \mathcal{U},$$

where $\mathbf{U}_{fp} = [\mathbf{u}_{fp,0}, \mathbf{u}_{fp,M}, \dots, \mathbf{u}_{fp,M(N_s-1)}]$. The solution returns the optimal foot placement sequence. Only the first value $\mathbf{u}_{fp,0}$ in the sequence is applied. The sets \mathcal{X} and \mathcal{U} constraining the states and control inputs are described next.

B. Constraint Sets

The state constraint set \mathcal{X} is the union of the mechanical safety set $\mathcal{X}^{\text{mech}}$ and the ground friction cone $\mathcal{X}^{\text{slip}}$. The foot placement safety set \mathcal{U} is also used to prevent foot collisions, most importantly in the lateral direction. The mechanical safety and foot placement safety sets are constructed as box constraints related to the geometrical limitations of the given robot.

The ground friction cone is based on the approximate 3D-ALIP dynamics. In this model, the ground reaction force is applied collinearly through the contact leg since the point mass moves parallel to the ground plane. Taking advantage of the known slope of the terrain, we can derive the resultant tangent and normal forces with respect to the ground for both x and y components to be

$$\begin{bmatrix} F_{T_x} \\ F_{N_x} \\ F_{T_y} \\ F_{N_y} \end{bmatrix} = \begin{bmatrix} \cos \alpha_x & 0 & -\sin \alpha_x \\ \sin \alpha_x & 0 & \cos \alpha_x \\ 0 & \cos \alpha_y & -\sin \alpha_y \\ 0 & \sin \alpha_y & \cos \alpha_y \end{bmatrix} \begin{bmatrix} F_x \\ F_y \\ F_z \end{bmatrix}. \quad (13)$$

From the motion constraints, we can also derive the relative force ratios

$$\begin{aligned} F_{x/z} &= \frac{F_x}{F_z} = \frac{x_c}{k_x x_c + k_y y_c + z_H} \\ F_{y/z} &= \frac{F_y}{F_z} = \frac{y_c}{k_x x_c + k_y y_c + z_H}. \end{aligned} \quad (14)$$

We combine this with a Coulomb static friction constraint ($F_{T_x} \leq \mu F_{N_x}$) between the component tangent and normal vectors to compute the slip constraints on x_c and y_c .

$$\begin{aligned} (1 - \mu \tan \alpha_x) F_{x/z} &\leq \tan \alpha_x + \mu \\ (1 - \mu \tan \alpha_y) F_{y/z} &\leq \tan \alpha_y + \mu. \end{aligned} \quad (15)$$

For known k_x , k_y , and μ , a set of (conditional) linear inequalities in x_c and y_c can be implemented. For simpler cases of pure forward and sideways walking, the inequalities simplify to

$$\begin{aligned} |x_c| &\leq \frac{(\mu + k_x)z_H}{1 - \mu k_x} \\ |y_c| &\leq \frac{(\mu + k_x)z_H}{1 - \mu k_x}. \end{aligned} \quad (16)$$

Clearly, this is not an exact friction slip constraint due to the simplifications of using the 3D-ALIP for ground reaction force estimation. However, it can be combined with an under-approximation of the friction coefficient μ to enable safer foot placements.

C. Cost Design

The cost function is the sum of a running cost and a terminal cost, with non-zero weights at step transitions, that is, $Q_i = \mathbf{0}, \forall i \notin \{0, M, 2M, \dots, (N_s-1)M\}$. Given a desired longitudinal angular momentum $L^{y,\text{des}}$ and step width W , we can use the solutions of (6) to compute the

desired state of the corresponding periodic orbit.

$$\begin{aligned} x_c(T_s) &= \cosh(\ell T_s) x_c(0) + \frac{1}{mz_H \ell} \sinh(\ell T_s) L^y(0) \\ y_c(T_s) &= \cosh(\ell T_s) y_c(0) - \frac{1}{mz_H \ell} \sinh(\ell T_s) L^x(0) \\ L^x(T_s) &= -mH\ell \sinh(\ell T_s) y_c(0) + \cosh(\ell T_s) L^x(0) \\ L^y(T_s) &= mz_H \ell \sinh(\ell T_s) x_c(0) + \cosh(\ell T_s) L^y(0) \end{aligned} \quad (17)$$

With the assumption of conservation of angular momentum about the contact point, we substitute $L^{y,des} = L^y(0) = L^y(T_s)$, $L^x(0) = -L^x(T_s)$, and $y_c(0) = W/2$ into (17) and solve the resultant linear system of equations.

$$\begin{aligned} x_c^{des} &= x_c(T_s) = \frac{1}{mz_H \ell} \tanh(\ell T_s/2) L_y^{des} \\ y_c^{des} &= \frac{1}{2} \text{sgn(stance)} W \\ L^{x,des} &= -\frac{1}{2} \text{sgn(stance)} mH\ell W \tanh(\ell T_s/2) + L^{x,offset} \end{aligned} \quad (18)$$

where sgn(stance) is +1 or -1 for left stance or right stance, respectively. As in [16], an offset is added to $L^{x,des}$ in order to account for lateral movement.

The terminal cost Q_f is computed as the optimal cost-to-go by solving the Discrete-Time Algebraic Riccati Equation for an entire step trajectory including impact, combining (6) and (7). This selection of terminal cost ensures recursive feasibility via Bellman's principle of optimality [30].

IV. VIRTUAL CONSTRAINTS AND FOOT PLACEMENT IMPLEMENTATION ON CASSIE

The computed foot placement solution is implemented on the high DoF bipedal robot Cassie Blue² through the use of specially designed virtual constraints. As documented in [16], an important feature of the 3D-ALIP model is that the mass of the swing leg and its corresponding momentum are accounted for in L^x and L^y .

Cassie is a 32 kg, 20 DoF biped robot actuated at ten joints. Each leg has seven joints, five of which are actuated while the remaining two are constrained by springs [31]. To achieve a desired foot placement, we must define the control variables for Cassie Blue and generate their reference trajectories. The nine control variables and the corresponding references are defined as follows

$$h = \begin{bmatrix} \text{torso pitch} \\ \text{torso roll} \\ \text{stance hip yaw} \\ \text{swing hip yaw} \\ p_{\text{COM}_{\text{proj}} \rightarrow \text{COM}}^z \\ p_{\text{st} \rightarrow \text{sw}}^x \\ p_{\text{st} \rightarrow \text{sw}}^y \\ p_{\text{st} \rightarrow \text{sw}}^z \\ \text{absolute swing toe pitch} \end{bmatrix} \quad (19)$$

²We have omitted the implementation and simulation of foot placement on the 3D-ALIP robot as the results are trivial due to the fact that a massless swing foot can achieve any position within the constraint set instantaneously for any step frequency.

$$h_d(s) := \begin{bmatrix} 0 \\ 0 \\ (1-s)h_3^{init} - s(\frac{1}{2}\Delta\psi) \\ (1-s)h_4^{init} + s(\frac{1}{2}\Delta\psi) \\ z_H \\ \frac{1}{2}[(1+\cos(\pi s))h_6^{init} + (1-\cos(\pi s))p_{\text{st} \rightarrow \text{sw}}^{x,des}] \\ \frac{1}{2}[(1+\cos(\pi s))h_7^{init} + (1-\cos(\pi s))p_{\text{st} \rightarrow \text{sw}}^{y,des}] \\ \beta_1 s^2 + \beta_2 s + \beta_3 \\ \tan(\alpha_x) \end{bmatrix}. \quad (20)$$

The desired reference trajectories are parametrized by a time-based phase variable $s = T_s - t/T_s$ where t is the time since last impact. We set the reference values for torso pitch, torso roll to be constant and zero. To enable turning one-half of the total desired turn angle $\Delta\psi$ at end of step is set as the reference position for both stance and swing yaw motor joints at the end of the current step. The reference absolute swing toe pitch angle is adjusted to align with the given terrain slope. The output $p_{\text{COM}_{\text{proj}} \rightarrow \text{COM}}^z$ represents the constant height parameter z_H , between the center of mass and the ground. With inclusion of the known slope values, it can be equivalently represented as the quantity $(p_{\text{st} \rightarrow \text{COM}}^z - k_x p_{\text{st} \rightarrow \text{COM}}^x - k_y)$.

Outputs, $p_{\text{st} \rightarrow \text{sw}}^{x,y}$ are set equal to the MPC foot placement solution $\mathbf{u}_{fp,0}$ described in (12). The z component of $p_{\text{st} \rightarrow \text{sw}}$ can be easily computed with the knowledge of k_x and k_y . We use sinusoidal references for the x and y components and a parabola for the z component parametrized by the initial and final heights of the swing leg determined by foot placement. The *init* superscript of all h_i^{init} denotes the value of each output at the beginning of each new step.

An input-output linearization method was used in simulation to validate these constraints for achieving desired foot placement locations. However due to model inaccuracies and state estimation noise, we implement an inverse kinematics and passivity-based control schema on the physical robot for improved tracking performance [17].

V. EXPERIMENTAL IMPLEMENTATION AND RESULTS

A. Controller Settings

The controller was coded in C++ and run on Cassie's secondary computer, in a Linux environment. Foot placement updates were sent over UDP at 1 kHz. The planning horizon of the MPC controller was set to four (robot) steps with a step period of 0.3 seconds and an intra-step time discretization of 10 ms. The QP resulting from the MPC formulation was code-generated using CasADi [32]. We used the virtual constraints of Sect. IV in all of the tests.

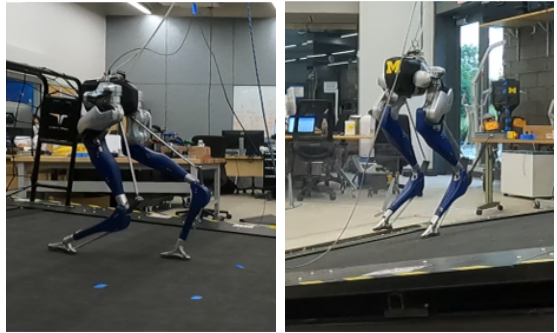
B. Results

The controller was implemented on Cassie Blue and evaluated in a number of situations that are itemized below.

- **Inclined walking.** Cassie walked forward on a treadmill inclined at 6° at a maximum speed of 1.5 m/s, and also walked laterally at a maximum speed of 0.5 m/s on a stationary treadmill inclined at 13°. When we tried the



(a) Forward walking at 1 m/s with a transition onto a stationary treadmill inclined at 13° .
(b) Lateral walking at 0.5 m/s with a transition onto a stationary treadmill inclined at 13° .



(c) Forward walking at 1.5 m/s on a treadmill inclined at 6° .
(d) Lateral walking at 0.5 m/s on a treadmill inclined at 13° .



(e) Forward walking at 1 m/s on wet, grassy slope inclined at 22° .

Fig. 3: Images from a variety of experiments performed with Cassie Blue using the foot placement controller discussed in this paper.

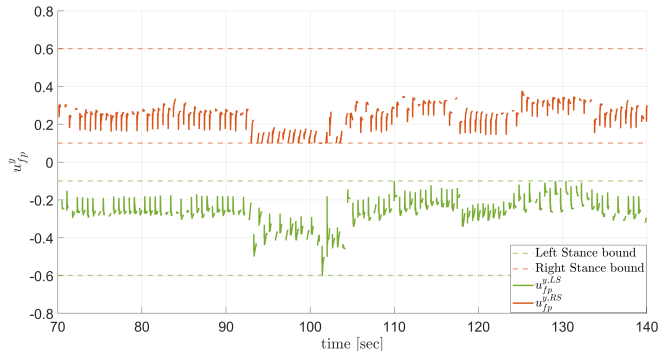


Fig. 4: Sequence of lateral foot placement solutions given by the MPC optimization problem during a lateral walking experiment. At $t = 92$ s the commanded lateral velocity was decreased causing the foot placement to deviate from its nominal periodic trajectory. We show that the constraints are satisfied in order to avoid foot collision and hyper-extension.

lateral walking with the one-step ahead controller of [16], which does not actively constrain the workspace of the legs, the robot tripped and fell.

- **Transitioning from Flat Ground to an Incline.** In this experiment, an operator sent the slope information to Cassie at the transition. Performance relied heavily on the timing and accuracy to which the operator was able to switch the estimated ground slope with respect the body frame of the robot at the exact moment that Cassie crossed the transition threshold. While these transitions were not ideal, due to operator error, a noticeable improvement of maintaining a constant COM height with respect to the ground was seen compared to [16].
- **Rapid Changes in Forward and Lateral Velocity.** In order to validate the foot placement constraints imposed by the MPC problem posed in Sec. III, we show the lateral foot placement value remains inside the foot placement safety set \mathcal{U} . This set is dependent upon stance leg choice and the solutions indeed lie within the set as shown in Fig. 4.
- **Walking Forward and Sideways up a 22° Grassy Slope.** We test the robustness of our control method by having Cassie Blue walk up an uneven, sloped hill with an estimated incline of 22° . We were successful in walking up the slope in the longitudinal direction at 1 m/s and the lateral direction at 0.3 m/s.

VI. CONCLUSIONS AND FUTURE WORK

This paper extended the controller based on one-step ahead prediction of angular and a constant CoM height [16] in three ways. First, the 3D-ALIP model was derived to allow the robot's center of mass to exhibit piecewise planar motion. Second, a four-step ahead MPC formulation of the controller was provided, which importantly, also included the intra-step dynamics at 10 ms intervals so that realistic workspace and terrain-aware constraints in the MPC formulation. Lastly, a novel set of virtual constraints was created that allowed us to realize the assumed CoM properties on a physical robot.

Currently, the performance of the robot is dependent on the ability of the operator to provide in real time an estimated terrain slope with respect to the body frame of the robot. This needs to come automatically from a perception system, as in [4]. When the slope is estimated accurately, the robot is very stable while walking with lateral and longitudinal velocity on sloped ground. In future work, we plan to: (a) explore the effects of different horizon lengths; (b) look at further relaxing the assumptions on the low-dimensional model (e.g., zero dynamics) to allow nonlinear terms; and (c) integrate the controller with a reactive planner.

ACKNOWLEDGMENT

Toyota Research Institute provided funds to support this work. Funding for J. Grizzle was in part provided by NSF Award No. 2118818. The authors thank Margaret Eva Mungai, Jennifer Humanchuk, and Jianyang Tang for their help in experiments. The experiments in the paper were conducted on Cassie Maize, thanks to a loan by the ROAHM Lab.

REFERENCES

[1] Omur Arslan and Daniel E Koditschek. Sensor-based reactive navigation in unknown convex sphere worlds. *The International Journal of Robotics Research*, 38(2-3):196–223, 2019.

[2] Santiago Paternain, Daniel E Koditschek, and Alejandro Ribeiro. Navigation functions for convex potentials in a space with convex obstacles. *IEEE Transactions on Automatic Control*, 63(9):2944–2959, 2017.

[3] Jiunn-Kai Huang and Jessy W Grizzle. Efficient anytime clif reactive planning system for a bipedal robot on undulating terrain. *arXiv preprint arXiv:2108.06699*, 2021.

[4] Jiunn-Kai Huang, Yukai Gong, Dianhao Chen, Jinze Liu, Minzhe Li, Jianyang Tang, Lu Gan, Ray Zhan, Wami Ogunbi, and Jessy Grizzle. Fully Autonomous on the Wave Field 2021. <https://youtu.be/gE3Y-2Q3gco>, 2021.

[5] John Wurts, Jeffrey L Stein, and Tulga Ersal. Collision imminent steering at high speeds on curved roads using one-level nonlinear model predictive control. *IEEE Access*, 9:39292–39302, 2021.

[6] Fabian Jenelten, Takahiro Miki, Aravind E Vijayan, Marko Bjelonic, and Marco Hutter. Perceptive locomotion in rough terrain–online foothold optimization. *IEEE Robotics and Automation Letters*, 5(4):5370–5376, 2020.

[7] Jia-chi Wu and Zoran Popović. Terrain-adaptive bipedal locomotion control. *ACM Transactions on Graphics (TOG)*, 29(4):1–10, 2010.

[8] Matthew J Powell, Huihua Zhao, and Aaron D Ames. Motion primitives for human-inspired bipedal robotic locomotion: walking and stair climbing. In *2012 IEEE International Conference on Robotics and Automation*, pages 543–549. IEEE, 2012.

[9] Katie Byl and Russ Tedrake. Metastable walking machines. *Int. J. Rob. Res.*, 28:1040–1064, August 2009.

[10] Hongkai Dai and Russ Tedrake. Planning robust walking motion on uneven terrain via convex optimization. In *Humanoid Robots (Humanoids), 2016 IEEE-RAS 16th International Conference on*, pages 579–586. IEEE, 2016.

[11] Brent Griffin and Jessy Grizzle. Nonholonomic virtual constraints and gait optimization for robust walking control. *The International Journal of Robotics Research*, page 0278364917708249, 2016.

[12] Zhaoming Xie, Patrick Clary, Jeremy Dao, Pedro Morais, Jonathan Hurst, and Michiel Panne. Learning locomotion skills for cassie: Iterative design and sim-to-real. In *Conference on Robot Learning*, pages 317–329. PMLR, 2020.

[13] Kaveh Akbari Hamed, Jeesop Kim, and Abhishek Pandala. Quadrupedal locomotion via event-based predictive control and qp-based virtual constraints. *arXiv preprint arXiv:2004.06858*, 2020.

[14] Shuji Kajita, Fumio Kanehiro, Kenji Kaneko, Kazuhito Yokoi, and Hirohisa Hirukawa. The 3d linear inverted pendulum mode: A simple modeling for a biped walking pattern generation. In *Proceedings 2001 IEEE/RSJ International Conference on Intelligent Robots and Systems. Expanding the Societal Role of Robotics in the the Next Millennium (Cat. No. 01CH37180)*, volume 1, pages 239–246. IEEE, 2001.

[15] Xiaobin Xiong, Jenna Reher, and Aaron Ames. Global position control on underactuated bipedal robots: Step-to-step dynamics approximation for step planning. *arXiv preprint arXiv:2011.06050*, 2020.

[16] Yukai Gong and Jessy Grizzle. One-step ahead prediction of angular momentum about the contact point for control of bipedal locomotion: Validation in a lip-inspired controller. In *IEEE International Conference on Robotics and Automation*, 2021.

[17] Yukai Gong and Jessy Grizzle. Zero dynamics, pendulum models, and angular momentum in feedback control of bipedal locomotion. *arXiv preprint arXiv:2105.08170*, 2021.

[18] Hirofumi Miura and Isao Shimoyama. Dynamic walk of a biped. *The International Journal of Robotics Research*, 3(2):60–74, 1984.

[19] Jerry Pratt, John Carff, Sergey Drakunov, and Ambarish Goswami. Capture point: A step toward humanoid push recovery. In *2006 6th IEEE-RAS international conference on humanoid robots*, pages 200–207. IEEE, 2006.

[20] Johannes Englsberger, Christian Ott, Máximo A Roa, Alin Albu-Schäffer, and Gerhard Hirzinger. Bipedal walking control based on capture point dynamics. In *2011 IEEE/RSJ International Conference on Intelligent Robots and Systems*, pages 4420–4427. IEEE, 2011.

[21] Ting Wang and Christine Chevallereau. Stability analysis and time-varying walking control for an under-actuated planar biped robot. *Robotics and Autonomous Systems*, 59(6):444 – 456, 2011.

[22] Xiaobin Xiong and Aaron D Ames. Orbit characterization, stabilization and composition on 3d underactuated bipedal walking via hybrid passive linear inverted pendulum model. In *2019 IEEE/RSJ International Conference on Intelligent Robots and Systems (IROS)*, pages 4644–4651. IEEE, 2019.

[23] Jacob Reher, Eric A Cousineau, Ayonga Hereid, Christian M Hubicki, and Aaron D Ames. Realizing dynamic and efficient bipedal locomotion on the humanoid robot durus. In *2016 IEEE International Conference on Robotics and Automation (ICRA)*, pages 1794–1801. IEEE, 2016.

[24] Xingye Da and Jessy Grizzle. Combining trajectory optimization, supervised machine learning, and model structure for mitigating the curse of dimensionality in the control of bipedal robots. *The International Journal of Robotics Research*, 38(9):1063–1097, 2019.

[25] Shuji Kajita, Fumio Kanehiro, Kenji Kaneko, Kiyoshi Fujiwara, Kensuke Harada, Kazuhito Yokoi, and Hirohisa Hirukawa. Biped walking pattern generation by using preview control of zero-moment point. In *ICRA*, volume 3, pages 1620–1626, 2003.

[26] Akihito Sano and Junji Furusho. Realization of natural dynamic walking using the angular momentum information. In *Proceedings., IEEE International Conference on Robotics and Automation*, pages 1476–1481. IEEE, 1990.

[27] Matthew J Powell, Wen-Loong Ma, Eric R Ambrose, and Aaron D Ames. Mechanics-based design of underactuated robotic walking gaits: Initial experimental realization. In *2016 IEEE-RAS 16th International Conference on Humanoid Robots (Humanoids)*, pages 981–986. IEEE, 2016.

[28] M. H. Raibert. *Legged robots that balance*. MIT Press, Mass., 1986.

[29] J.K. Hodgins and M. H. Raibert. Adjusting step length for rough terrain locomotion. *IEEE Transactions on Robotics and Automation*, 7(3):289–98, June 1991.

[30] Francesco Borrelli, Alberto Bemporad, and Manfred Morari. *Predictive control for linear and hybrid systems*. Cambridge University Press, 2017.

[31] Y. Gong, R. Hartley, X. Da, A. Hereid, O. Harib, J. Huang, and J. Grizzle. Feedback control of a cassie bipedal robot: Walking, standing, and riding a segway. In *2019 American Control Conference (ACC)*, pages 4559–4566, 2019.

[32] Joel A E Andersson, Joris Gillis, Greg Horn, James B Rawlings, and Moritz Diehl. CasADi – A software framework for nonlinear optimization and optimal control. *Mathematical Programming Computation*, 11(1):1–36, 2019.